Hierarchical Organization of the Human Auditory Cortex Revealed by Functional Magnetic Resonance Imaging

C.M. Wessinger[1,2], J. VanMeter[1], B. Tian[1], J. Van Lare[1], J. Pekar[1,3], and J.P. Rauschecker[1]

Abstract

■ The concept of hierarchical processing—that the sensory world is broken down into basic features later integrated into more complex stimulus preferences—originated from investigations of the visual cortex. Recent studies of the auditory cortex in nonhuman primates revealed a comparable architecture, in which core areas, receiving direct input from the thalamus, in turn, provide input to a surrounding belt. Here functional magnetic resonance imaging (fMRI) shows that the human auditory cortex displays a similar hierarchical organization: pure tones (PTs) activate primarily the core, whereas belt areas prefer complex sounds, such as narrow-band noise bursts. ■

INTRODUCTION

Sensory areas in the cerebral cortex of nonhuman primates have long been thought to be organized into a core receiving direct input from the principal thalamic relay nuclei, and into belt areas surrounding this core (Pandya & Sanides, 1973). This anatomical scheme has been elaborated in great detail for the auditory cortex in the superior temporal gyrus (STG) of the rhesus monkey (Galaburda & Pandya, 1983). Use of histochemical markers has recently permitted the refinement and expansion of the distinction between core and belt areas (Hackett, Stepniewska, & Kaas, 1998; Jones, Dell'Anna, Molinari, Rausell, & Hashikawa, 1995; Morel, Garraghty, & Kaas, 1993). Concomitant neurophysiological evidence confirms that neurons in the core areas, such as the primary auditory cortex (A1) and the rostral area (R), respond well to pure tones (PTs) and are narrowly tuned to frequency, whereas normal responsiveness at later stages depends on the integrity of the core (Rauschecker, Tian, Pons, & Mishkin, 1997). Three cochleotopically organized areas on the STG, the anterolateral (AL), middle lateral (ML), and caudolateral (CL) areas, have been identified on the basis of their responses to band-passed noise (BPN) bursts (Rauschecker, Tian, & Hauser, 1995). Such stimuli greatly enhance the response of neurons in these lateral belt areas compared to PTs. Further, these neurons are tuned to the center frequency as well as bandwidth of the noise bursts. Given that lateral belt areas receive their major input from core areas (Hackett et al., 1998), these physiological findings support the notion of a hierarchical organization within the auditory cortex of primates (Kaas, Hackett, & Tramo, 1999; Rauschecker, 1998), similar to that found in the visual cortex (Felleman & van Essen, 1991; Desimone & Ungerleider, 1989; Zeki & Shipp, 1988).

Studies of physiological activity in the human auditory cortex have been performed with a variety of techniques, including positron emission tomography (PET) (Lockwood et al., 1999; Lauter, Herscovitch, Formby, & Raichle, 1985) and magnetoencephalography (MEG) (Pantev et al., 1995), but most of these techniques cannot localize auditory cortical areas in individual subjects with sufficient detail. These problems can be overcome by using functional magnetic resonance imaging (fMRI), which permits noninvasive visualization and localization of stimulus-specific functional activity directly on the underlying individual brain anatomy. An early fMRI study demonstrated frequency-specific responses and tonotopic organization in the posterior Heschl's gyrus (Wessinger, Buonocore, Kussmaul, & Mangun, 1997). More recent fMRI investigations of auditory processing employing a wider range of stimuli, including tones, nonspeech noise, meaningless speech sounds, single words, and narrative text, have conclusively demonstrated stimulus-specific differential activation within human auditory cortex (Scheich et al., 1998; Binder et al., 1997, 2000; Grady et al., 1997). However, as in prior PET studies (Price et al., 1996; Démonet et al., 1992; Zatorre, Evans, Meyer, & Gjedde, 1992; Wise et al., 1991; Petersen, Fox, Posner, Mintun, & Raichle, 1988),

[1] Georgetown Institute for Cognitive and Computational Sciences, Georgetown University Medical Center, [2] Dartmouth College and Medical School, [3] Johns Hopkins University and Kennedy Krieger Institute

the experimental design and stimulus sets employed were intended to be most informative with regard to speech and language processing. In the present study, we utilize a stimulus design with energy-matched sound bursts differing in bandwidth to test the core–belt model of cortical organization. The results provide a surprisingly clear answer with regard to the hierarchical organization of the human auditory cortex and

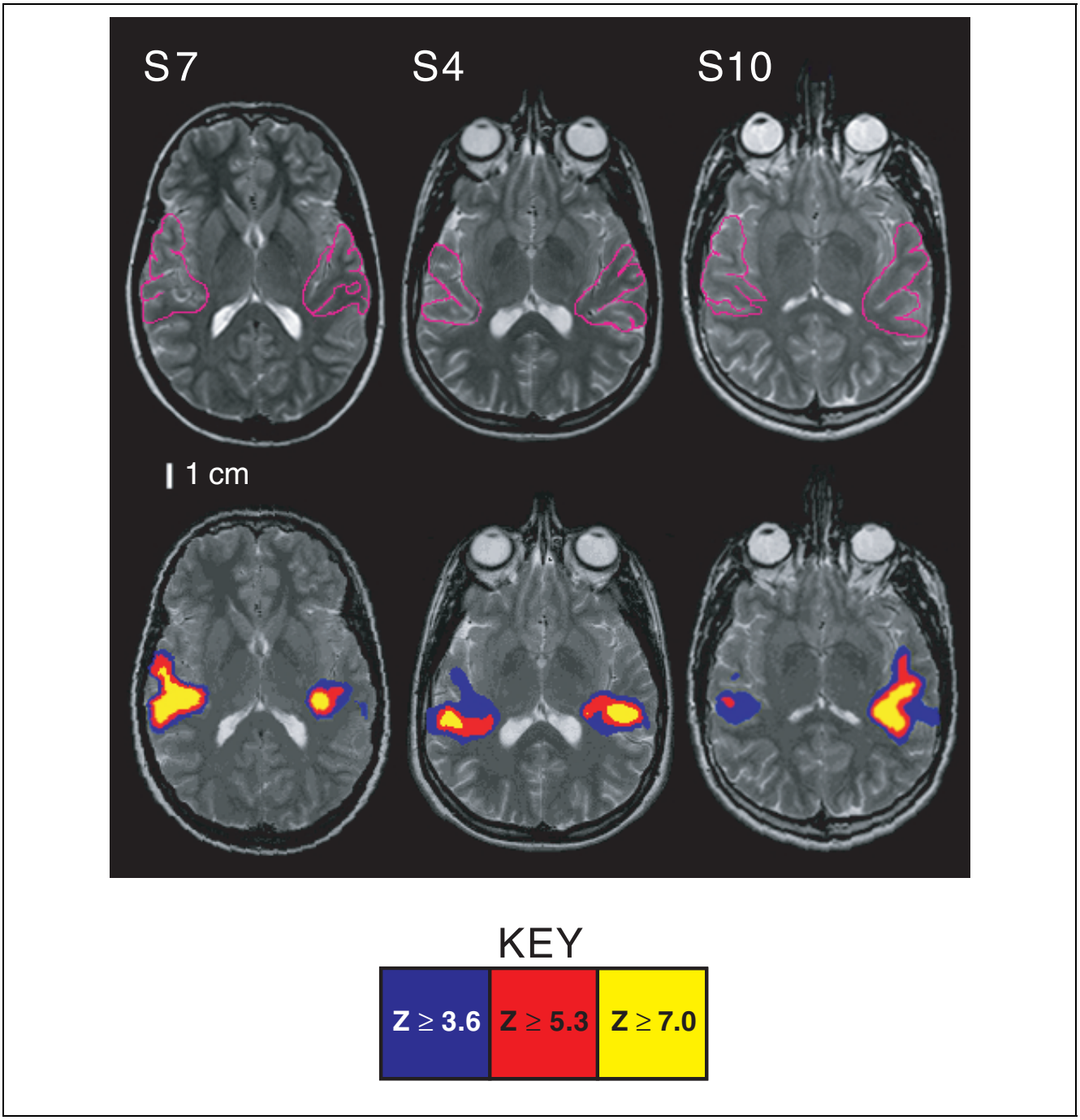

Figure 1. Oblique-axial slices approximately parallel to the STP showing anatomical images (top) and regions of activation (bottom) produced by auditory stimulation in three representative subjects. The overall activation maps were produced by combining all 192 time-points (i.e., all the acoustic stimuli) from individual subjects for analysis (see Methods for details). Thresholded *Z* maps are coregistered and overlaid on coplanar anatomical images from each individual subject. The key at the bottom of the figure indicates the *Z* score associated with each color plotted. In the anatomical images, Heschl's region, consisting of multiple transverse gyri (Penhune et al., 1996; Rademacher et al., 1993), is outlined in purple. Since the border of Heschl's region is not well defined in the anterolateral direction, its outline is continued all the way to the edge of the slice. Note the left/right asymmetry in some cases. All images are displayed in radiological coordinates such that the left hemisphere is on the right, and anterior is at the top.

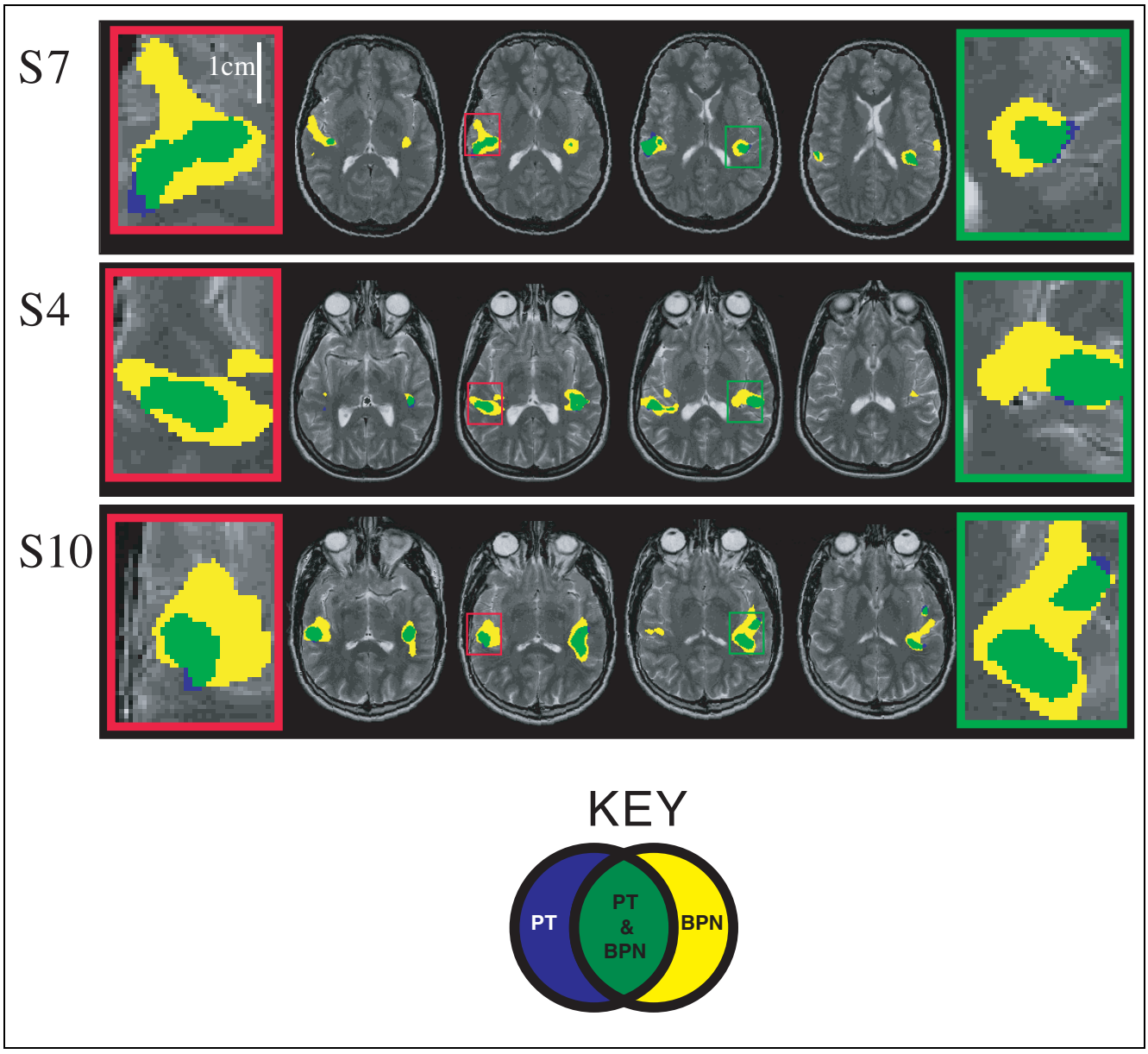

Figure 2. Bandwidth-specific data from the same subjects as in Figure 1. Areas shown in blue represent activation by PT, yellow represents activation by BPN bursts, and green represents overlap between PT and BPN activation. PT stimuli activate only a core region of the auditory cortex, whereas surrounding belt areas are only activated by BPN bursts. Enlarged views of representative bandwidth distributions are shown for each subject (outlined in red and green for the right and left hemisphere, respectively). The slices are arranged left-to-right in an inferior-to-superior manner. Activation is plotted with $Z \geq 4.2$.

relate the functional activation to individual cortical anatomy by means of structural MRI.

RESULTS

In order to ensure adequate activation of the auditory cortex, we first computed an overall activation Z map by comparing the scans with auditory stimuli to the scans without them, using all 192 time-points. All but one of our 12 subjects showed significant stimulus-correlated activation ($p \leq .05$, Bonferroni-corrected). The one subject with inadequate activation was dropped from subsequent analyses. Activation was primarily restricted to contiguous areas within the four or five slices surrounding the STG. Thresholded Z maps were overlaid on coplanar anatomical images from each individual subject. Comparison of functional and structural scans revealed that regions of activation within the supratemporal plane (STP) of individual subjects were concentrated around the one or two transverse gyri of Heschl (Penhune, Zatorre, MacDonald, & Evans, 1996; Rademacher, Caviness, Steinmetz, & Galaburda, 1993), subsequently referred to as Heschl's region (Penhune et al., 1996). The Z maps often showed a characteristic crescent-shaped form with the most significant Z values ($Z \geq 7.0$) in the

center, surrounded by zones with smaller Z values ($Z \geq 3.6$ and $Z \geq 5.3$; Figure 1).

Volumes were subsequently sorted into different groups for analysis by stimulus type. Firstly, PT and BPN stimuli were combined across all three frequencies resulting in two bandwidth-specific data sets, each composed of 96 volumes. Secondly, the PT and BPN stimuli with the same center frequency were combined into three frequency-specific data sets (high, medium, low), each composed of 64 volumes. It is important to note that all stimuli were energy-matched on the basis of their root-mean-square (RMS) values to equalize intensity.

Analysis of the data in terms of stimulus bandwidth (''complexity'') revealed multiple activation foci, bilaterally, in the auditory cortex of individual subjects. Coplotting the statistical maps based on PT and BPN data sets shows that the PT stimuli generally result in smaller, more restricted foci, while the BPN stimuli produce larger, more extensive regions of activation (Figure 2). Thus, regions that are activated by both PT and BPN stimuli are surrounded by regions that respond only to BPN bursts. In most cases, the PT foci are contained completely within the BPN activation regions and coincide with the regions of highest Z values shown in Figure 1. While they form mostly contiguous areas of activation, they break up into separate zones in some of the subjects.

Individual activation volumes of all 11 subjects are given in Table 1. A two-factor analysis of variance of stimulus complexity (PT vs. BPN) by hemisphere (left vs. right) demonstrates a significantly greater activation volume for BPN than for PT stimuli ($F = 6.087$, $p \leq .02$). There was a trend towards greater activation in the left hemisphere, but this difference did not reach significance ($F = 2.705$, $p \leq .1$).

Analysis of the data in terms of frequency-specific stimulus parameters in individual subjects also revealed multiple activation foci for each of the low-, medium-, and high-frequency data sets suggestive of multiple tonotopic maps. In particular, we found that Heschl's region (Penhune et al., 1996), as determined from the coregistered structural scans, often contained two mirror-symmetric frequency gradients. Unfortunately, activation by tones of a single frequency was too weak and inconsistent to pass our statistical criteria. Activation with the broader-band BPN bursts, on the other hand, often resulted in large areas of overlap, occluding the known tonotopic organization of the auditory cortex. Regions of overlap activated by all three frequency bands were generally found in the center of the crescent-shaped activation areas (see cover illustration).

Table 1. Activation Volumes (in mm^3) Calculated for Each Stimulus Type in the Left and Right Hemisphere for Individual Subjects ($p \leq .0005$)

Subject	*PT-left*	*PT-right*	*BPN-left*	*BPN-right*
S1	913	0	5,875	3,827
S2	0	0	2,210	0
S3	4,312	2,156	3,557	1,940
S4	2,318	1,779	6,414	7,708
S5	0	0	862	0
S6	0	1,294	0	4,150
S7	6,252	4,743	9,163	8,355
S8	1,078	1,348	4,743	6,630
S9	3,234	4,150	4,797	2,102
S10	4,258	3,234	12,989	7,546
S11	3,934	3,180	2,910	916
Avg	2,391	1,989	4,865	3,924
SD	2,150	1,675	3,744	3,186

PT = pure tone; BPN = band-passed noise; Avg = mean volume; *SD* = standard deviation.

DISCUSSION

The present data demonstrate that PTs activate only a restricted region of the human auditory cortex. This region is surrounded by areas activated only by stimuli with greater spectral complexity, such as BPN, but not by tones. This organization is highly reminiscent of the core–belt distinction made for the auditory cortex in nonhuman primates (Kaas et al., 1999; Rauschecker et al., 1995; Rauschecker, 1998). In fact, the above relationship has been used to define core and belt areas physiologically in rhesus monkeys. Thus, we can conclude that the same basic organizational pattern holds for both primate species. The core areas in the present study coincide also with areas of strongest activation, as assessed by their Z values, which indicates a lower activation threshold also consistent with observations from monkey electrophysiology. Furthermore, we found that this region generally falls within the anatomical landmarks used to delimit the core of the auditory cortex along Heschl's gyri in individual subjects.

The identification of collateral representations adjacent to the core areas in our study is consistent with the notion of belt regions in macaque monkeys (Kaas et al., 1999; Rauschecker, 1998). The organization and position of these collateral representations varied across subjects. The use of more specific, spectrally complex, and time-varying stimuli, in conjunction with refined functional imaging methods (such as a smaller field of view resulting in smaller voxel size, or the use of a higher field-strength magnet resulting in a greater signal-to-noise ratio), should allow even more higher-order auditory areas to be characterized in the future.

The main result of our study in terms of similarity between human and nonhuman primates was the fact that PT stimuli rarely activated areas outside a well-defined core region, while BPN stimuli activated both core and belt regions. It appears unlikely that this result could be explained merely by linear summation, i.e., the activation of a larger number of frequencies along the tonotopic axis. This would not lead to an equal expansion of the activated region orthogonal to this axis, as observed here. The differential activation by PT and BPN stimuli cannot be due to thresholding or smoothing either, because these processes equally affect both conditions. Although the absolute size of activated regions may change slightly as a result of image processing, the relative sizes of PT- and BPN-activated regions would stay about the same. Finally, because all stimuli were energy-matched, the present data cannot be explained by different signal energy. Rather, our results suggest strongly that large-scale nonlinear spectral integration, based on convergence of afferents from the core region (Kaas et al., 1999; Hackett et al., 1998), occurs in the belt areas, which renders PTs largely ineffective outside the core (Rauschecker et al., 1995; Rauschecker, 1998). Single neurons in the lateral belt of nonhuman primates (but not in the primary-like core areas) show precisely the same kind of spectral integration; their responses are greatly enhanced by the use of BPN bursts compared to PTs and are tuned to specific bandwidths (Rauschecker, 1998; Rauschecker et al., 1995). These identical findings in both nonhuman primates and man challenge the traditional notion of the auditory system as a quasi-linear Fourier analyzer that is best tested by the use of tonal stimuli. Instead, by far the largest part of the auditory cortex outside of the primary core areas requires complex sounds for activation.

The identification of core and belt regions is also consistent with previous human electrophysiological and anatomical studies. In an earlier surface electrode recording study in surgical patients, a core auditory region with at least two lateral areas is described (Celesia, 1976). A more recent study of patients with temporal lobe lesions that combines behavioral data with morphometric imaging techniques successfully parcels Heschl's region into separate posterior and anterior processing areas (Penhune et al., 1996), and cytoarchitectonic results report the existence of three separate areas, two of them primary-like (Morosan et al., 1999). The average size of our core activation is in excellent agreement with these morphometric studies: respective volumes for the left and right hemispheres in our study are 2391 and 1989 mm^3 (Table 1) and 2172 and 1329 mm^3 for what is termed the ''primary auditory cortical region'' (PAC-r) in the study of Penhune et al., (1996).

Like other neuroimaging techniques, such as PET, fMRI does not directly report on neuronal activity. Rather, regional activity is assessed by measuring relative changes in the MR signal over time. The signal changes are due to local changes in the concentration of deoxyhemoglobin, caused by local hemodynamic responses, which are thought to result from local neuronal processing changes as a function of stimulus manipulations within the experimental design. Several reviews have described the successful application of fMRI techniques when localizing a variety of sensory and cognitive brain functions within the cerebral cortex (Le Bihan & Karni, 1995; Cohen & Bookheimer, 1994; DeYoe, Bandettini, Neitz, Miller, & Winans, 1994). By employing similar techniques in the auditory domain, we have now used fMRI to successfully localize regions of the cortex activated by stimuli of different complexity, clearly demonstrating distributed hierarchical processing within the human auditory cortex, comparable to that found for the visual system of nonhuman primates (Felleman & van Essen, 1991; Desimone & Underleider, 1989; Zeki & Shipp, 1988).

In conclusion, our data strongly support the notion of a hierarchy of multiple cortical areas, organized serially and in parallel (Rauschecker et al., 1995, 1997), within the human auditory cortex. The core of this processing hierarchy is located in the posterior (and medial) aspects of Heschl's region, with later processing stages spreading both laterally and medially from there. This processing hierarchy functions much like the processing hierarchy of the visual system where later stages build on the outputs of the early stages (Felleman & van Essen, 1991; Desimone & Ungerleider, 1989; Zeki & Shipp, 1988). Finally, in light of the data reported here and other evidence gathered in our laboratory (Morad et al., 1999; Wessinger et al., 1998), we propose that this hierarchical system participates in the early processing of a broad variety of complex sounds, including human speech. How nonspeech and speech sound processing is differentially compartmentalized within these areas and whether or not such information is ultimately relayed to different processing modules specialized for distinct classes of complex sounds awaits further experimentation.

METHODS

Twelve healthy, right-handed subjects (average age = 25; six males) with normal hearing participated with informed consent. During each functional scan, subjects listened passively to one of six different stimulus sets. These sets consisted of either PTs with a frequency of 0.5, 2, or 8 kHz, or BPN bursts with the same logarithmically spaced center frequencies and a bandwidth of one octave (i.e., from 0.35–0.7, 1.4–2.8, and 5.6–11.2 kHz, respectively). All stimuli were 500 msec in duration including 50-msec rise/fall times to minimize on/offset artifacts of the speaker and presented at a rate of 1 Hz during the ''stimulus-on'' intervals of the functional scans. The stimuli were digitally synthesized on a PC using ''Signal'' (Engineering Design, Belmont, MA), con-

verted to Macintosh sound file format and presented using ''MacStim'' (David Darby, Melbourne, Australia) from a PowerBook 520c. The PowerBook was interfaced with a custom air conduction sound system that delivered the signals binaurally to the subjects with silicone-cushioned headphones specifically designed to isolate the subject from the scanner noise (Resonance Technology, Van Nuys, California). The RMS values of the stimuli were matched and presented at 75 dB SPL as measured with a B&K (Brüel & Kjaer, Naerum, Denmark) 0.5-in. condenser microphone (No. 4133, free-field) and a B&K Precision Sound Level Meter (No. 2235).

Magnetic resonance images were obtained using a Siemens Magnetom Vision 1.5-Tesla whole-body scanner equipped with a gradient booster overdrive enabling echo-planar imaging (EPI) with an echo time (TE) of 40 msec. Four subjects underwent 12 functional runs consisting of four 32-sec cycles divided into two 16-sec ''stimulus-on'' and ''stimulus-off'' epochs. During six runs each PT and BPN bursts were the on-stimuli. The other eight subjects underwent six functional runs consisting of eight 32-sec cycles divided into two 16-sec ''stimulus-on'' and ''stimulus-off'' epochs. There were three runs each with PT and BPN bursts as the on-stimuli. All functional runs were preceded by three pre-experimental baseline volumes designed to establish energy saturation. In all runs, the ambient scanner noise served as the off-stimulus. In total, after discarding the baseline volumes, 192 volumes were collected for analysis in each of the subjects. Every functional volume consisted of 13 oblique-axial slices tilted transverse to coronal by approximately 11.5°. This tilt was designed to orient the slices roughly parallel to the STP and provide better views of Heschl's gyri. Four-millimeter thick slices were collected with an interslice gap of 10% with a 64 × 64 matrix in a 240-mm field of view resulting in a nominal voxel size of 3.75 × 3.75 × 4.4 mm^3.

One concern with using fMRI to study audition is the noise generated by the scanner during data acquisition. In order to minimize functional activation associated with the scanner sound, sparse-sampling techniques were used that allow for silence between volume acquisitions (Edmister, Talavage, Ledden, & Weisskoff, 1999; Hall et al., 1999; see also Wessinger, et al., 1997) that is, repetition time (TR) was 8,000 msec, and volume collection was accomplished during the first 2,000 msec. High-resolution anatomical coplanar T2 images (nominal voxel size = 0.94 × 0.94 × 4.4 mm) were obtained during the same scanning session, in order to facilitate the localization of activation foci on anatomical brain structures, such as Heschl's gyri.

Changes in local MRI signal related to local cortical activity via the blood-oxygenation level dependent (BOLD) effect were used to assess functional activation. MEDx (Sensor Systems, Sterling, VA) was used both for data analysis and image visualization. Given that the data were collected across multiple functional runs for each subject, it was necessary to correct for both inter- and intrarun head motion. The first nonbaseline scan was used as the standard image to which all 192 time-points were registered using the Automated Image Registration (AIR) algorithm (Woods, Mazziotta, & Cherry, 1993), as implemented in MEDx. All EPI images were smoothed using a Gaussian filter with a full width half maximum (FWHM) of 7.5 × 7.5 × 8.8 mm (twice the voxel size). Image intensities were regressed to the mean using linear detrending in order to remove signal drift associated with fluctuations of the B_0 magnetic field. Noise outside the area of the brain was excluded by thresholding each image at 20% of the maximum intensity within the volume. Activation was assessed by computing a correlation coefficient between signal intensity changes and a box-car reference waveform at each voxel (Bandettini, Jesmanowicz, Wong, & Hyde, 1993). Correlation coefficient maps were constructed and converted into *Z* maps. Additionally, a cluster analysis of the *Z* maps that considered both the spatial extent and magnitude of the activation was used (Friston, Worsley, Frackowiak, Mazziotta, & Evans, 1994). The transformation matrix derived from the image registration was applied to the *Z* maps using trilinear interpolation. This additional interpolation accounts for the apparent higher resolution of the functional data when overlaid on the T2 images.

Acknowledgments

This work was supported by NIH grant RO1-DC-03489 (J.P.R.) and DOD grant DAMD17-93-V-3018. We would like to thank Drs. G. Liu and C. Platenberg for their valuable input concerning the fMRI parameters, as well as J. Agnew, N. Athale, A. Durham, D. Kim, C. Marvel, A. Morad, and S. Yargici for help with experimental design, stimulus creation, and data processing. C.M.W. would like to acknowledge the support of Drs. J. Bharucha and M.S. Gazzaniga while completing this manuscript. S. Courtney, D. Hall, B. Horwitz, and I. Johnsrude provided helpful comments on an earlier draft.

Reprint requests should be sent to Josef P. Rauschecker, Georgetown Institute for Cognitive and Computational Sciences, Georgetown University Medical Center, 3970 Reservoir Rd, NW, Washington, DC 20007-2197. Email: rauscheckerj@giccs.georgetown.edu.

The data reported in this experiment have been deposited in the National fMRI Data Center (http://www.fmridc.org). The accession number is 2-2001-111A4.

REFERENCES

Association for Research in Otolaryngology Abstracts, 20, 27

Bandettini, P. A., Jesmanowicz, A., Wong, E. C., & Hyde, J. S. (1993). Processing strategies for time-course data sets in functional MRI of the human brain. *Magnetic Resonance in Medicine, 30,* 161–173.

Binder, J. R., Frost, J. A., Hammeke, T. A., Cox, R. W., Rao, S. M., & Prieto, T. (1997). Human brain language areas identified by functional magnetic resonance imaging. *Journal of Neuroscience, 17,* 353–362.

Binder, J. R., Frost, J. A., Hammeke, T. A., Bellgowan, P. S. F., Springer, J. A., Kaufman, J. N., & Possing, E. T. (2000). Human temporal lobe activation by speech and nonspeech sounds. *Cerebral Cortex, 10,* 512–528.

Celesia, G. G. (1976). Organization of auditory cortical areas in man. *Brain, 99,* 403–414.

Cohen, M. S., & Bookheimer, S. Y. (1994). Localization of brain function using magnetic resonance imaging. *Trends in Neurosciences, 17,* 268–277.

Démonet, J. F., Chollet, F., Ramsay, S., Cardebat, D., Nespoulous, J. L., Wise, R., Rascol, A., & Frackowiak, R. (1992). The anatomy of phonological and semantic processing in normal subjects. *Brain, 115,* 1753–1768.

Desimone, R., & Ungerleider, L. G. (1989). Neural mechanisms of visual processing in monkeys. In F. Boller & J. Grafman (Eds.), *Handbook of neuropsychology,* vol. 2 (pp. 267–298). New York: Elsevier.

DeYoe, E. A., Bandettini, P., Neitz, J., Miller, D., & Winans, P. (1994). Functional magnetic resonance imaging (FMRI) of the human brain. *Journal of Neuroscience Methods, 54,* 171–187.

Edmister, W. B., Talavage, T. M., Ledden, P. J., & Weisskoff, R. M. (1999). Improved auditory cortex imaging using clustered volume acquisitions. *Human Brain Mapping, 7,* 89–97.

Felleman, D. J., & van Essen, D. C. (1991). Distributed hierarchical processing in the primate cerebral cortex. *Cerebral Cortex, 1,* 1–47.

Friston, K. J., Worsley, K. J., Frackowiak, R. S. J., Mazziotta, J. C., & Evans, A. C. (1994). Assessing the significance of focal activations using their spatial extent. *Human Brain Mapping, 1,* 210–220.

Galaburda, A. M., & Pandya, D. N. (1983). The intrinsic architectonic and connectional organization of the superior temporal region of the rhesus monkey. *Journal of Comparative Neurology, 221,* 169–184.

Grady, C. L., et al., (1997). Attention-related modulation of activity in primary and secondary auditory cortex. *NeuroReport, 8,* 2511–2516.

Hackett, T. A., Stepniewska, I., & Kaas, J. H. (1998). Subdivisions of auditory cortex and ipsilateral cortical connections of the parabelt auditory cortex in macaque monkeys. *Journal of Comparative Neurology, 394,* 475–495.

Hall, D. A., Haggard, M. P., Akeroyd, M. A., Palmer A. R., Summerfield, A. Q., Elliott, M. R., Gurney, E. M., & Bowtell, R. W. (1999). ''Sparse'' temporal sampling in auditory fMRI. *Human Brain Mapping, 7,* 213–223.

Jones, E. G., Dell'Anna, M. E., Molinari, M., Rausell, E., & Hashikawa, T. (1995). Subdivisions of macaque monkey auditory cortex revealed by calcium-binding protein immunoreactivity. *Journal of Comparative Neurology, 362,* 153–170.

Kaas, J. H., Hackett, T. A., & Tramo, M. J. (1999). Auditory processing in primate cerebral cortex. *Current Opinion in Neurobiology, 9,* 164–170.

Lauter, J. L., Herscovitch, P., Formby, C., & Raichle, M. E. (1985). Tonotopic organization in human auditory cortex revealed by positron emission tomography. *Hearing Research, 20,* 199–205.

Le Bihan, D., & Karni, A. (1995). Applications of magnetic resonance imaging to the study of human brain function. *Current Opinion in Neurobiology, 5,* 231–237.

Lockwood, A. H., Salvi, R. J., Coad, M. L., Arnold, S. A., Wack, D. S., Murphy, B. W., & Burkard, R. F. (1999). The functional anatomy of the normal human auditory system: responses to 0.5 and 4.0 kHz tones at varied intensities. *Cerebral Cortex, 9,* 65–76.

Morad, et al., (1999). *Neuroimage, 9,* S996.

Morel, A., Garraghty, P. E., & Kaas, J. H. (1993). Tonotopic organization, architectonic fields, and connections of auditory cortex in macaque monkeys. *Journal of Comparative Neurology, 335,* 437–459.

Morosan, et al., (1999). *Neuroimage, 9,* S141.

Pandya, D. N., & Sanides, F. (1973). Architectonic parcellation of the temporal operculum in rhesus monkey and its projection pattern. *Zeitschrift für Anatomie und Entwicklungsgeschichte, 139,* 127–161.

Pantev, C., Bertrand, O., Eulitz, C., Verkindt, C., Hampson, S., Schuierer, G., Elbert, T. (1995). Specific tonotopic organizations of different areas of the human auditory cortex revealed by simultaneous magnetic and electric recordings. *Electroencephalography and Clinical Neurophysiology, 94,* 26–40.

Penhune, V. B., Zatorre, R. J., MacDonald, J. D., & Evans, A. C. (1996). Interhemispheric anatomical differences in human primary auditory cortex: Probabilistic mapping and volume measurement from magnetic resonance scans. *Cerebral Cortex, 6,* 661–672.

Petersen, S. E., Fox, P. T., Posner, M. I., Mintun, M., & Raichle, M. E. (1988). Positron emission tomographic studies of the cortical anatomy of single-word processing. *Nature, 331,* 585–589.

Price, C. J., et al., (1996). Hearing and saying. The functional neuro-anatomy of auditory word processing. *Brain, 119,* 919–931.

Rademacher, J., Caviness, V. S., Jr., Steinmetz, H., & Galaburda, A. M. (1993). Topographical variation of the human primary cortices: Implications for neuroimaging, brain mapping, and neurobiology. *Cerebral Cortex, 3,* 313–329.

Rauschecker, J. P. (1998). Cortical processing of complex sounds. *Current Opinion in Neurobiology, 8,* 516–521.

Rauschecker, J. P., Tian, B., & Hauser, M. (1995). Processing of complex sounds in the macaque nonprimary auditory cortex. *Science, 268,* 111–114.

Rauschecker, J. P., Tian, B., Pons, T., & Mishkin, M. (1997). Serial and parallel processing in rhesus monkey auditory cortex. *Journal of Comparative Neurology, 382,* 89–103.

Scheich, H., Baumgart, F., Gaschler-Markefski, B., Tegeler, C., Tempelmann, C., Heinze, H. J., Schindler, F., & Stiller, D. (1998). Functional magnetic resonance imaging of a human auditory cortex area involved in foreground–background decomposition. *European Journal of Neuroscience, 10,* 803–809.

Wessinger, C. M., Buonocore, M. H., Kussmaul, C. L., & Mangun, G. R. (1997). Tonotopy in human auditory cortex examined with functional magnetic resonance imaging. *Human Brain Mapping, 5,* 18–25.

Wessinger, C. M., Van Lare, J. E., Tian, B., Van Meter, J. W., Pekar, J., & Rauschecker, J. P. (1998). Activation within human auditory cortex correlated with stimulus complexity. *Soc Neurosci. Abstr., 24,* 400.

Wise, R., Chollet, F., Hadar, U., Friston, K., Hoffner, E., & Frackowiak, R. (1991). Distribution of cortical neural networks involved in word comprehension and word retrieval. *Brain, 114,* 1803–1817.

Woods, R. P., Mazziotta, J. C., & Cherry, S. R. (1993). MRI–PET registration with automated algorithm. *Journal of Computer-Assisted Tomography, 17,* 536–546.

Zatorre, R. J., Evans, A. C., Meyer, E., & Gjedde, A. (1992). Lateralization of phonetic and pitch discrimination in speech processing. *Science, 256,* 846–849.

Zeki, S., & Shipp, S. (1988). The functional logic of cortical connections. *Nature, 335,* 311–317.